Acta Biochim Biophys Sin (2010): 195–201 | © The Author 2010. Published by ABBS Editorial Office in association with Oxford University Press on behalf of the Institute of Biochemistry and Cell Biology, Shanghai Institutes for Biological Sciences, Chinese Academy of Sciences. DOI: 10.1093/abbs/gmq004.

A quantitative study on morphological responses of osteoblastic cells to fluid shear stress

Xiaoli Liu, Xu Zhang, and Imshik Lee*

State Key Laboratory of Bioactive Materials, School of Physics, Nankai University, Tianjin 300071, China
*Correspondence address. Tel: +86-22-23494411. E-mail: ilee@nankai.edu.cn

Fluid shear stress (FSS) is widely explored regarding its influence on osteoblasts. *In vitro* studies have shown that the cytoskeleton is very important in cellular responses to FSS. However, morphological changes, which would reflect the cytoskeleton changes as well as other cellular responses, were rarely quantitatively studied in the past years. Therefore, FSS-induced morphological changes in osteoblasts were quantified in this study. Real-time rapid morphological responses were observed by exposing osteoblasts to FSS with magnitude of 1.2, 1.6, and 1.9 Pa for 1 h. Afterward, osteoblast actin cytoskeleton was labeled with rhodamine phalloidin and observed using fluorescence microscopy. The results showed that 1.6 and 1.9 Pa FFS resulted in significant cellular elongation and reorientation along the direction of fluid flow. Besides, along with the enhancement of FSS magnitude, cytoskeleton aggregated more remarkably. Furthermore, extracellular Ca^{2+}-depleted fluid flow was also used to stimulate osteoblasts for 1 h with magnitude of 1.6 and 1.9 Pa. No morphological change was observed after removing extracellular calcium. Our study suggested that the level of FSS from 1.2 to 1.9 Pa is capable of influencing cellular morphology, and extracellular calcium might play a role in osteoblasts' response to FSS stimulation.

Keywords fluid shear stress; osteoblast; morphology; cytoskeleton; image analysis

Received: September 9, 2009 Accepted: December 14, 2009

Introduction

It is well known that bone cells are exposed to a complex environment which exerts several types of mechanical stress such as stretching stress [1,2], fluid shear stress (FSS) [3], and hydrostatic pressure [4]. All these types of stress have influence on bone metabolism, especially on bone formation and remodeling [5,6]. Since Reich *et al*. [7] revealed the biological response of bone cells under FSS in 1990, how FSS takes effects on osteoblasts has been widely explored and significant results have been obtained, including the uploading of Ca^{2+} signals [8,9]; increase in cAMP, prostaglandins [10], and NO [11]; increase in gene expressions of *COX-2* and *c-fos* [12]; overexpression of cross-linking proteins such as vimentin, α-actinin, and filamin [13]; enhancement of osteoblasts proliferation and differentiation [14,15]; and enhancement of integrin-regulated gene expression which is related to bone formation [16]. In particular, cytoskeleton was considered to be very important in cellular responses to FSS stimulation. Tensegrity theory published in 1997 indicated that cytoskeleton was the key of cells to sense mechanical stimulations [17]. Likewise, it is well accepted that the cytoskeleton plays important roles in keeping cell morphology and transferring molecular signals [18,19]. Therefore, investigation in changes of cytoskeleton is useful for clarifying how osteoblasts respond to FSS stimulation.

Since cell morphology was regulated by cytoskeleton, thus certain morphological changes may indirectly reflect the responses of upstream signals at molecular level, e.g. calcium signals. Accordingly, biological responses, especially changes of cytoskeleton, could be quantified by morphological measurement. Although some studies have reported morphological changes in osteoblasts under stimulation of FSS [3,12,13,20], little information on quantitative study was available in the past years. Horikawa *et al*. [21] reported the relationship between duration of FSS and morphological changes in osteoblasts in 2000. However, no study to date has included the analysis of the relationship between magnitude of FSS and morphological changes. Since quantitative investigation of morphological changes would be helpful in clarifying the influences of FSS on osteoblasts, the aim of this study is to explore the effects of FSS on cell morphology quantitatively.

Theoretical modeling predicted that shear stress in the range 0.8–3.0 Pa most approaches to FSS *in vivo* [22]. Additionally, FSS from 1.0 to 2.0 Pa was usually applied to experiments *in vitro* [14,16,20]. Thus, FSS of 1.2, 1.6, and 1.9 Pa were chosen to examine the morphological changes in osteoblasts in this study. Rapid morphological responses were observed during the stimulations. Besides, FSS-induced

actin-cytoskeleton changes were quantified by using rhodamine-phalloidin imaging techniques. Osteoblasts elongated and reoriented along the direction of the fluid flow. Also, with the increase in FSS magnitude, actin-cytoskeleton aggregated more apparently. Furthermore, morphological change in osteoblasts was not observed after removing extracellular calcium, implying the significance of extracellular calcium in osteoblasts' response to FSS stimulation.

Materials and Methods

Cell culture

The calvariae of Wistar rat (3–5-day-old, Chinese Academy of Medical Sciences, Tianjin, China) was used for isolating osteoblast-like cells. Procedures of cell isolation and cell culture were described in our earlier report [2]. Cells were grown in RPMI 1640 medium (10.4 g/L RPMI 1640, 2 g/L $NaHCO_3$, 5.96 g/L HEPES, 0.05 g/L penicillin G, 0.1 g/L streptomycin sulfate, pH 7.2), and cultured at 37°C in an MCO175 incubator (SANYO Electric Biomedical Co., Ltd, Osaka, Japan) containing 5% CO_2. In the present experiments, cells were subcultured on glass slides (32 mm × 24 mm) at $2.5–3 \times 10^4$ cells/cm^2. Fluid flow was applied 48 h after subculture so that cells were 80–90% confluent at the time of experimentation.

Flow chamber and experiment

As shown in **Fig. 1**, a parallel-plate flow chamber was used to introduce fluid flow over the cells. The fluid-flow setup consisted of a parallel-plate flow chamber and a recirculating flow circuit. This circuit included a variable-speed peristaltic pump and a reservoir with RPMI 1640 medium maintained at 37°C with 5% CO_2. To investigate the role of extracellular calcium in response to shear stress, 1.5 mM ethylene glycol tetra-acetic acid (EGTA) was supplemented into RPMI 1640 medium to produce Ca^{2+}-depleted medium. This system produces laminar flow over a cell monolayer. A flow rate was chosen to yield a τ-value of 1.2, 1.6 or 1.9 Pa by using $\tau = 6Q\mu/bh^2$, where Q is the flow rate, μ the medium viscosity, b the channel width, and h the channel height. Control cells were kept under static conditions with the same culture medium at 37°C with 5% CO_2.

In real-time observation, this system was equipped with an Axio Observer D1 inverted microscope (Zeiss, Berlin, Germany) and pictures were recorded every 5 min for 1 h using DU-897D-CS0-BV CCD system (Andor, London, UK).

Fluorescence observation and image analysis

Rhodamine phalloidin was used to label cytoskeletal F-actin according the method described [23]. Cells were washed in PBS, fixed with 4% paraformaldehyde (diluted in PBS) for 30 min and then rinsed twice in PBS. PBS containing 0.5% Triton X-100 (*v*/*v*) was used to permeate the membrane for 30 min. Then cells were rinsed twice in PBS. Rhodamine-phalloidin mixed solution (2.4%) was used to label osteoblasts actin cytoskeleton (200 μl for each glass slide). After labeling (10 min, 25°C), the coverslips were washed twice in PBS and observed with fluorescence microscope using a 40× oil lens with the MetaMorph 7.1 software (Universal Imaging,

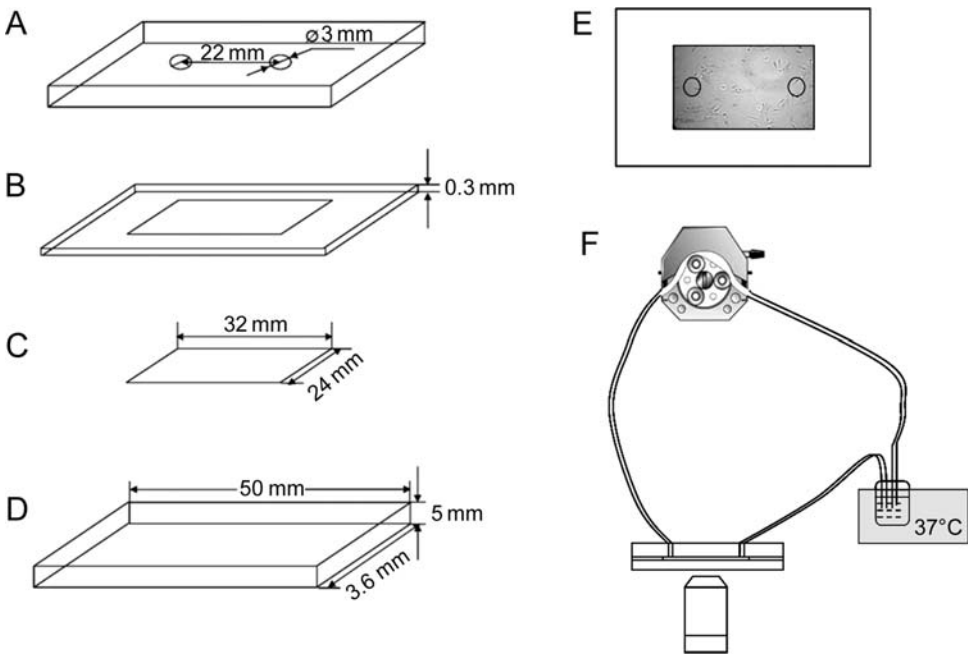

Figure 1 A schematic illustration of the parallel-plate flow chamber used to induce FSS The parallel plates are comprised of (A) a quartz slide with an inlet and a outlet, (B) a thin rubber silastic gasket with uniform thickness, (C) a cover slide on which osteoblasts were cultured, and (D) a quartz slide of the same size as (A). (E) An overhead view of the assembled fluid cell. (F) The assembled system. The sizes of all parts were shown in this figure.

Downingtown, USA) capable of cell-by-cell analysis. The exposure time was 100 ms. Measurement was recorded for 20–25 cells selected randomly within one slide of a culture and repeated for several cultures.

We used two shape factors, r and Circularity, to quantify cell shape. r is the ratio of cell length (defined along the major axis) to cell width (defined along the minor axis). Circularity is defined as $4\pi A/P^2$ for quantifying the degree of cell's circularity, where A is the area and P the perimeter. The other two parameters, Angle and AngleSD, were used to represent cell orientation. Parameter Angle is the absolute value of the angular orientation when compared with the direction of the FSS (a smaller number in Angle indicates that cell oriented near the direction of the shear stress). AngleSD is the standard deviation of Angle in one group, which was used to reflect the orientational distribution of the cells. Additionally, the fluorescence intensity (FI), which is proportional to the concentration of labeled F-actin for not too large absorption of the emitted fluorescence light, was used to quantify the content of labeled F-actins.

Statistical analysis

Statistical differences in the cell morphological parameters were determined by the Student's t-test and one-way ANOVA. Statistical significance was established at the $P < 0.05$ and all experimental analyses were performed blind.

Results

Real-time observation of cell morphology

In an applied stimulation of FSS, some cells (**Fig. 2**) elongated along the long axis of cell in the first 15 min and no dose-dependent characteristics were seen. Although not very distinct in phase contrast pictures, the trends of these cells to bulge and become more spindle-shaped could be seen, particularly in the highlighted regions (red arrows). FSS exerted in this experiment was 1.2 Pa [**Fig. 2(A–C)**], 1.6 Pa [**Fig. 2(D–F)**], and 1.9 Pa [**Fig. 2(G–I)**], respectively. Photos were recorded chronologically at a 5-min interval. After 15 min, no apparent morphological change was observed (data not shown). Since real-time morphological changes were observed, quantitative analysis was then conducted by using fluorescence microscopy.

Fluorescence observation and image analysis

F-actins of control cells were of clearly visible filamentous configuration [**Fig. 3(A)**]. After FSS stimulation for 1 h, the F-actins tended to arrange parallel to the long axis of cell [**Fig. 3(B)**], which was consistent with the result of real-time observation.

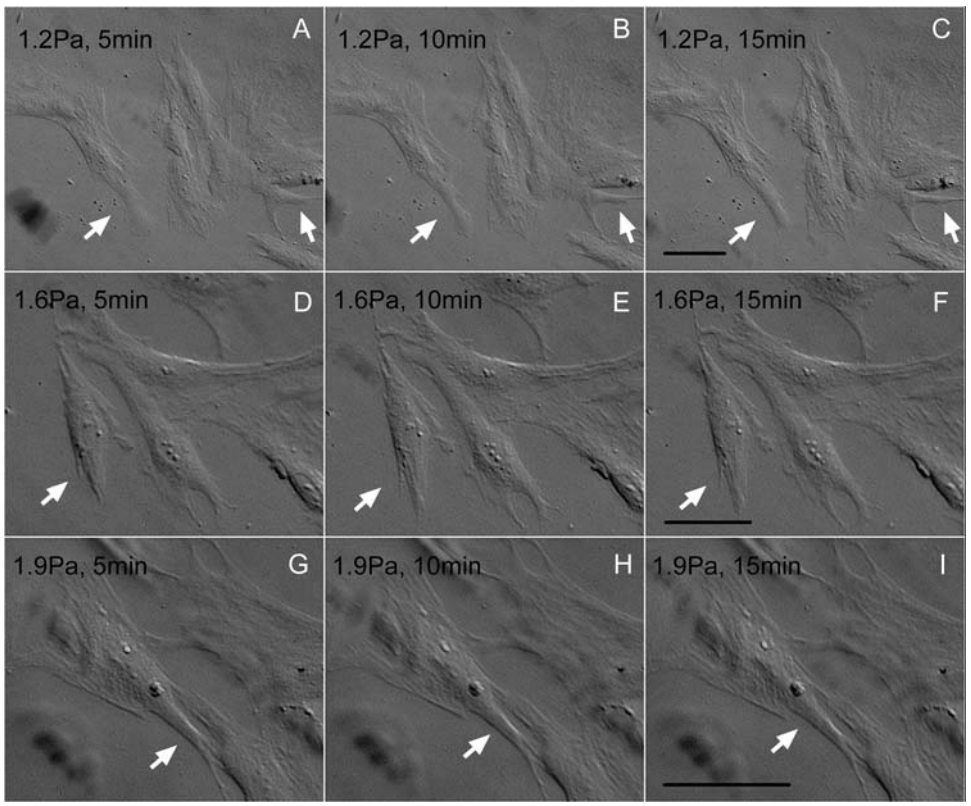

Figure 2 Real-time observation of cell shape under the stimulation of FSS with different magnitudes (A–C) show the cells under 1.2 Pa FSS for 5, 10 and 15 min, respectively. (D–F) show the cells under 1.6 Pa FSS for 5, 10, and 15 min, respectively. (G–I) show the cells under 1.9 Pa FSS for 5, 10, and 15 min, respectively. Cells tended to bulge and become more spindle shape (arrow) in the first 15 min of stimulation. Scale bar = 50 μm.

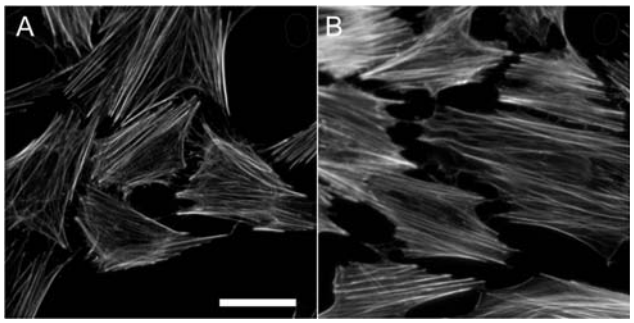

Figure 3 Fluorescence micrographs of cells labeled with rhodamine-phalloidin (A) control group, cells arranged randomly. (B) Cells after 1-h stimulation of 1.6 Pa FSS. The F-actins tended to arrange parallel to the long axes of cells and reorient into uniform direction. Scale bar = 50 μm.

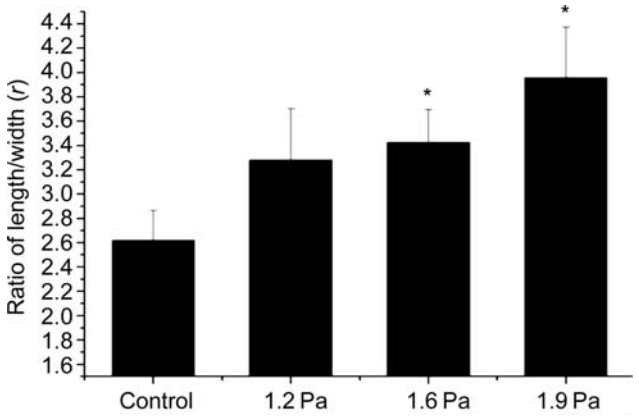

Figure 4 The length–width ratio *r* given as a function of FSS intensity After 1-h stimulation, both 1.6 and 1.9 Pa FSS resulted in significant increase in *r*, indicating the elongation of the osteoblastic cells. Data are the mean ± SE from three individual experiments. *$P < 0.05$ compared with control group.

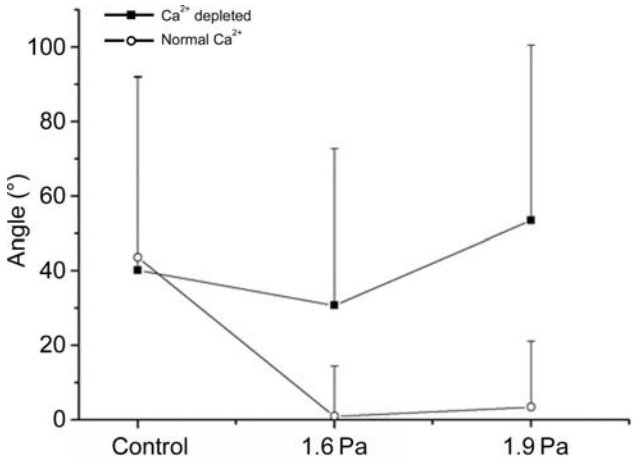

Figure 5 Comparison in changes of orientation parameters (Angle and AngleSD) between normal group and calcium-depleted group After 1-h stimulation, neither Angle nor AngleSD reduced distinctly in extracellular calcium-depleted group as in the normal group, which suggested that osteoblasts did not reorient under FSS without extracellular calcium. Data are the mean ± SD from three individual experiments.

Meanwhile, morphological information of the cells (*r*, Circularity, Angle, AngleSD) was measured (**Table 1**). In the control group, *r* was 2.619 ± 0.249, whereas Circularity was 0.312 ± 0.027 (a circularity value of 1.0 indicating a circular shape, and a smaller value indicating a more spindle-shaped cell). Correspondingly, cell Angle was 40.222 ± 16.345°. And less SD indicates more uniform cellular orientation, thus no evidence of preferred cell orientation was found, with the AngleSD being 51.686°.

Statistical analysis of the image data revealed significant increase in *r* of 1.6 Pa group ($P = 0.042$) and 1.9 Pa group ($P = 0.011$) (**Fig. 4** and **Table 1**). Also, 1.9 Pa stimulation resulted in apparent decrease ($P = 0.03$) in cell Circularity when compared with the control group (**Table 1**). Both enhancement of *r* and reduction in Circularity suggested that cell elongated and became more narrowly spindle-shaped after stimulation, especially under the stimulation of 1.9 Pa FSS. The same trend (i.e. increase in *r* and decrease in Circularity), though did not approach statistical significance ($P = 0.182$ for *r*, $P = 0.694$ for Circularity), could be seen in the 1.2-Pa group. On the other hand, significant reduction in Angle values after stimulations of 1.6 Pa ($P = 0.0005$) and 1.9 Pa ($P = 0.001$) are shown in **Table 1** and **Fig. 5** (versus control group). The Angle values of 1.6 Pa (0.906 ± 4.281) and 1.9 Pa (3.474 ± 5.573) were much smaller than that of control (40.222 ± 16.345), indicating that cells preferentially aligned along the direction of the shear stress. In addition, distinct decrease in AngleSD (control: 51.686; 1.6 Pa: 13.538; 1.9 Pa: 17.623) suggested that cells reoriented from random distribution to uniform orientation (**Figs. 3** and **5**).

Table 1 Morphological measurements of rhodamine-phalloidin stained osteoblasts after 1-h stimulation of FSS with different magnitudes

Group	*r*	Circularity	Angle (°)	AngleSD[a] (°)
Control	2.619 ± 0.249	0.312 ± 0.027	40.222 ± 16.345	51.686
1.2 Pa	3.281 ± 0.419	0.295 ± 0.031	25.778 ± 12.233	38.684
1.6 Pa	3.426 ± 0.271*	0.273 ± 0.013	0.906 ± 4.281**	13.538**
1.9 Pa	3.960 ± 0.414*	0.229 ± 0.020*	3.474 ± 5.573**	17.623**

Data are presented as the mean ± SE. *$P < 0.05$, **$P < 0.01$ versus control group. [a]AngleSD is the standard deviation of Angle in one group, see the 'Materials and Methods' section for detail. *r* is the ratio of cell length (defined along the major axis) to cell width (defined along the minor axis).

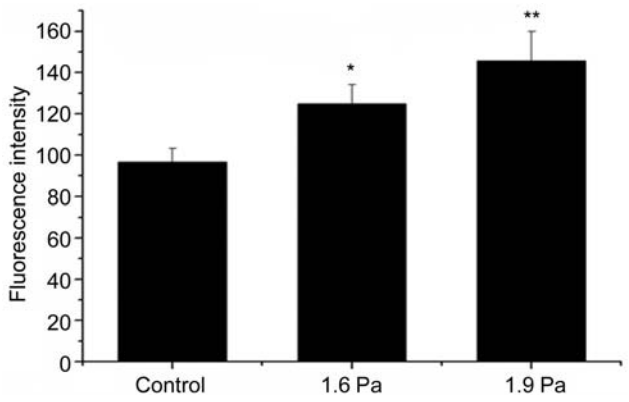

Figure 6 The FI given as a function of FSS intensity After 1-h stimulation, both 1.6 and 1.9 Pa FSS caused significant increase in FI, which implied the aggregation of the actin cytoskeleton. Data are the mean ± SE from three individual experiments. *$P < 0.05$ and **$P < 0.01$ compared with control group.

The FI of cytoskeleton was also measured (**Fig. 6**). Consistent with the influences on cell morphology, both 1.6 and 1.9 Pa stimulation resulted in significant increases ($P = 0.017$ in 1.6 Pa group, $P = 0.003$ in 1.9 Pa group) in FI compared with controls, which was indicative of aggregation of F-actin filaments. Overall, the data showed that the morphological change is dependent on the magnitude of FSS (**Table 1**, **Figs. 4** and **6**).

Extracellular Ca^{2+} depletion experiment

Since intensities of 1.6 and 1.9 Pa seemed to have robust effect on cell morphology as shown above, these two stimulations were applied in calcium-depleted experiment. As a result, no significant differences were found in cell shape factors in both 1.6 and 1.9 Pa groups comparing with the control group ($P > 0.05$, **Table 2**), nor were any changes in FI value observed (data not shown). Similarly, orientation parameters (Angle and AngleSD) showed no apparent change when compared with the control group ($P > 0.05$, **Table 2**). To more thoroughly illustrate the role of calcium, comparison in orientation parameters between normal medium and calcium-depleted medium was prepared (**Fig. 5**). The figure showed that both Angle and AngleSD did not reduce distinctly in Ca^{2+}-depleted group as in the control group, i.e. cells stimulated by 1.6 and 1.9 Pa FSS still distributed randomly without a preferential orientation.

Discussion

Cytoskeleton is well known to be important as the mechanical sensor of osteoblasts to FSS [3]. On the other hand, it is widely accepted that cytoskeletal elements, including microfilaments, microtubules, and intermediate filaments, are important in maintaining the normal shape of cell. There are two types of actins: F-actins in filamentous form and G-actins in free form, both of which are the basic component of microfilaments. Osteoblasts presented a trend of extension under the influence of FSS [12,13,21,24]. However, little work has been done to make further analysis on the change of cytoskeleton or morphology. Recently, it was shown that the cause of cytoskeleton changes might be the increase of anchor points [25], the release of intracellular Ca^{2+} induced by inositol 1,4,5-triphosphate (IP_3) [20] or the increase in linking proteins [13,26]. Also, it was reported that the changes in cytoskeleton might exert a function of transferring mechanical signaling into osteoblasts [12]. Though cytoskeleton of osteoblasts has been emphasized and studied, limited quantitative morphological research work, which would reflect cytoskeleton changes as well as other biological responses of cells, was published in the past years. Horikawa *et al*. [21] measured morphological changes in osteoblasts by exerting 10 dyn/cm^2 FSS on three groups of cells for 1, 6, and 12 h, respectively. As a result, cell elongation and $[Ca^{2+}]_i$ enhancement were observed in 1 h group. Besides, long-term FSS stimulation was concluded to have destructive effects on osteoblasts. In view of the report of Horikawa, 1-h stimulation was chosen in our experiment. Moreover, we explored morphological changes in osteoblasts by exerting FSS with different magnitudes. Also, we investigated the role of extracelluar Ca^{2+} on morphological changes in osteoblasts. Since we could only observe filamentous actins by phalloidin staining, other cytoskeletal elements were not studied in the present work.

Real-time observation suggested that the osteoblasts tended to elongate in the first 15 min of stimulations. Though not very obvious, the tendency of elongation

Table 2 Morphological measurements of rhodamine-phalloidin stained osteoblasts after 1-h stimulation of FSS with different magnitudes under extracellular calcium-depleted condition

Condition	*r*	Circularity	Angle (°)	AngleSD[a] (°)
Control	2.619 ± 0.249	0.312 ± 0.027	40.222 ± 16.345	51.686
1.6 Pa	2.4193 ± 0.209	0.353 ± 0.034	30.757 ± 10.821	41.913
1.9 Pa	2.4637 ± 0.183	0.345 ± 0.021	53.517 ± 11.390	46.961

Data are presented as the mean ± SE. [a]AngleSD is the standard deviation of Angle in one group, see the 'Materials and Methods' section for detail. *r* is the ratio of cell length (defined along the major axis) to cell width (defined along the minor axis).

implied a rapid response of osteoblasts to FSS stimulation (**Fig. 2**). Previously, a fast release of ATP in osteoblasts was observed in the first 15 min of FSS stimulation [27]. The release depended on L-type voltage-sensitive Ca^{2+} channel (L-VSCC) and the mechanosensitive, cation-selective channel (MSCC)-induced influx of extracelluar Ca^{2+}, which is the activator of mitogen-activated protein kinase (MAPK) pathway [28]. Therefore, we inferred without certainty that the rapid morphological response in osteoblasts we observed in this study might be related to the extracellular Ca^{2+} influx induced by the opening of these channels.

Most importantly, we used rhodamine-phalloidin labeling method to analyze morphological changes in osteoblasts. Coincident with the research of Horikawa *et al*. [21], osteoblasts extended along the long axis after stimulation (**Fig. 3**). Besides, we found that osteoblasts stimulated by FSS with larger magnitude presented more apparent morphological changes. Although there was not significant difference in the 1.2-Pa group compared with control group, we could also observe the extended trend of the cells (**Fig. 4**). These observations suggested that the targets of FSS were cytoskeleton F-actins and it was the structural changes of the filaments induced by FSS that obviously preceded the changes in the overall cell shape. On the other hand, cell orientation changed in coincidence with the change of cell shape. After stimulation, cells tended to redistribute along the direction of the fluid flow. Moreover, the larger the FSS was, the more uniformly the osteoblasts rearranged.

It was apparent from the discussion above that the morphological changes were dependent on the FSS magnitude and there seemed to be a threshold of osteoblasts in sensing FSS stimulation. In the research of cellular response to electromagnetic stimulation, 'window effect' was suggested [29–31], which means only to a certain range of stimulation can cells show biological responses. Meanwhile, mechanotransduction was also suggested to be induced by a similar rule [32]. Because bone adaptation to mechanical loading depends on the duration and the magnitude of the applied loads [33,34], it is reasonable to assume that the 'window effect' may exist in osteoblasts' response to FSS stimulation. As shown in **Fig. 6**, the increase in FI implied the aggregation of F-actins, which might result in the changes in shape and orientation of cells. Osteoblasts were considered to change cytoskeleton so as to resist negative impacts of FSS such as detachment and apoptosis [35]. Therefore, cytoskeleton aggregation-induced morphological changes might either effectively reduce the net force operating on cell surface or strengthen adhesion ability of the cells during stimulation. Furthermore, it was conceivable that other responses like overexpression of certain genes, enhancement of cell proliferation and increase in cell differentiation induced by FSS might also result from cellular resistance to the stimulation.

FSS-induced extracellular Ca^{2+} influx has been implicated as an important regulator to mediate the activity of integrins and F-actin cytoskeleton realignment. Extracellular Ca^{2+} was considered as a cofactor inducing intracellular calcium response [10], a stimulator of a fast vesicular ATP release [25], a supplement of intracellular calcium concentration [27], and a key to the activation of ERK1/2 pathway [28], during all the responses above osteoblasts were observed to realign along the direction of FSS. Others, however, argued that it was intracellular, not extracellular calcium that controlled cellular responses to FSS [20,21]. In order to test whether extracellular Ca^{2+} plays a role in the responses, we examined its effect from the view of cellular morphological change. After chelating extracellular calcium by 1.5 mM EGTA, neither morphological (shape and orientation) nor FI change was observed (**Table 2** and **Fig. 5**). From this point of view, extracellular calcium took influence on morphological response in osteoblasts to FSS. However, further researches about the influence of extracellular calcium or intracellular calcium on cellular morphology were not conducted in the present study. Thus, at this stage of investigation, it is not possible to say extracellular calcium was essential for osteoblasts in responding to FSS stimulation. However, it could be suggested that extracellular calcium, within the limitations of these experiments at least, was one of the factors affecting cellular responses to FSS stimulation. Our work quantitatively explored the influence of FSS on morphology of osteoblasts. Dose-dependent changes in shape and orientation were possibly induced by cytoskeleton aggregation and might relate to extracellular calcium influx. Further studies will be required to investigate the changes of cytoskeleton by real-time research, which, in our view, will be promising in revealing cellular responses to FSS stimulation.

Acknowledgements

We thank Dr Leiting Pan for his encouragement and assistance in the experiment.

Funding

This work was supported a grant from the Tianjin Natural Science Foundation (07JCYBJC12600).

References

1 Kaspar D, Seidl W, Neidlinger-Wilke C, Ignatius A and Claes L. Dynamic cell stretching increases human osteoblast proliferation and CICP synthesis but decreases osteocalcin synthesis and alkaline phosphatase activity. J Biomech 2000, 33: 45–51.

2 Zhang X, Liu XL, Sun JL, He SJ, Lee I and Pak HK. Real-time observations of mechanical stimulus-induced enhancements of mechanical properties in osteoblast cells. Ultramicroscopy 2008, 108: 1338–1341.

3 Myers KA, Rattner JB, Shrive NG and Hart DA. Osteoblast-like cells and fluid flow: cytoskeleton-dependent shear sensitivity. Biochem Biophys Res Commun 2007, 364: 214–219.
4 Diehl P, Mittelmeier W, Preissner KT, Goebel M, Gradinger R, Gollwitzer H and Eichelberg K, *et al*. Effect of high hydrostatic pressure on biological properties of extracellular bone matrix proteins. Int J Mol Med 2005, 16: 285–289.
5 Duncan RL and Turner CH. Mechanotransduction and the functional response of bone to mechanical strain. Calcif Tissue Int 1995, 57: 344–358.
6 Ingber DE. Mechanobiology and diseases of mechanotransduction. Ann Intern Med 2003, 35: 564–577.
7 Reich KM, Gay CV and Frangos JA. Fluid shear stress as a mediator of osteoblast cyclic adenosine monophosphate production. J Cell Physiol 1990, 143: 100–104.
8 Hung CT, Pollack SR, Reilly TM and Brighton CT. Real-time calcium response of cultured bone cells to fluid flow. Clin Orthop Relat Res 1995, 313: 256–269.
9 Donahue SW, Jacobs CR and Donahue HJ. Flow-induced calcium oscillations in rat osteoblasts are age, loading frequency, and shear stress dependent. Am J Physiol Cell Physiol 2001, 281: 35–41.
10 Hung CT, Allena FD, Pollacka SR and Brighton CT. Intracellular Ca^{2+} stores and extracellular Ca^{2+} are required in the real-time Ca^{2+} response of bone cells experiencing fluid flow. J Biomech 1996, 29: 1411–1417.
11 González O, Fong KD, Trindade MC, Warren SM, Longaker MT and Smith RL. Fluid shear stress magnitude, duration, and total applied load regulate gene expression and nitric oxide production in primary calvarial osteoblast cultures. Plast Reconstr Surg 2008, 122: 419–428.
12 Pavalko FM, Chen NX, Turner CH, Burr DB, Atkinson S, Hsieh YF and Qiu J, *et al*. Fluid shear-induced mechanical signaling in MC3T3-E1 osteoblasts requires cytoskeleton-integrin interactions. Am J Physiol Cell Physiol 1998, 275: 1591–1601.
13 Jackson WM, Jaasma MJ, Tang RS and Keaveny TM. Mechanical loading by fluid shear is sufficient to alter the cytoskeletal composition of osteoblastic cells. Am J Physiol Cell Physiol 2008, 295: 1007–1015.
14 Kapur S, Baylink DJ and Lau KH. Fluid flow shear stress stimulates human osteoblast proliferation and differentiation through multiple interacting and competing signal transduction pathways. Bone 2003, 32: 241–251.
15 Kapur S, Chen ST, Baylink DJ and Lau KH. Extracellular signal-regulated kinase-1 and -2 are both essential for the shear stress-induced human osteoblast proliferation. Bone 2004, 35: 525–534.
16 Lee DY, Yeh CR, Chang SF, Lee PL, Chien S, Cheng CK and Chiu JJ. Integrin-mediated expression of bone formation-related genes in osteoblast-like cells in response to fluid shear stress: roles of extracellular matrix, Shc, and mitogen-activated protein kinase. J Bone Miner Res 2008, 23: 1140–1149.
17 Ingber DE. Tensegrity: the architectural basis of cellular mechanotransduction. Annu Rev Physiol 1997, 59: 575–599.
18 Ingber DE. Cellular basis of mechanotransduction. Biol Bull 1998, 194: 323–325.
19 Wang JH and Thampatty BP. An introductory review of cell mechanobiology. Biomech Model Mechanobiol 2006, 5: 1–16.
20 Chen NX, Ryder KD, Pavalko FM, Turner CH, Burr DB, Qiu J and Duncan RL. Ca^{2+} regulates fluid shear-induced cytoskeletal reorganization and gene expression in osteoblasts. Am J Physiol Cell Physiol 2000, 278: 989–997.
21 Horikawa A, Okada K, Sato K and Sato M. Morphological changes in osteoblastic cells (MC3T3-E1) due to fluid shear stress: cellular damage by prolonged application of fluid shear stress. Tohoku J Exp Med 2000, 191: 127–137.
22 Bonewald LF. Mechanosensation and transduction in osteocytes. Bonekey Osteovision 2006, 3: 7–15.
23 Wieland T, Miura T and Seeliger A. Analogs of phalloidin. D-Abu2-Lys7-phalloin, an F-actin binding analog, its rhodamine conjugate (RLP) a novel fluorescent F-actin-probe, and D-Ala2-Leu7-phalloin, an inert peptide. Int J Pept Protein Res 1983, 21: 3–10.
24 Turner CH and Pavalko FM. Mechanotransduction and functional response of the skeleton to physical stress: the mechanisms and mechanics of bone adaptation. J Orthop Sci 1998, 3: 346–355.
25 Liedert A, Kaspar D, Blakytny R, Claes L and Ignatius A. Signal transduction pathways involved in mechanotransduction in bone cells. Biochem Biophys Res Commun 2006, 349: 1–5.
26 Thi MM, Kojima T, Cowin SC, Weinbaum S and Spray DC. Fluid shear stress remodels expression and function of junctional proteins in cultured bone cells. Am J Physiol Cell Physiol 2003, 284: 389–403.
27 Riddle RC and Donahue HJ. From streaming potentials to shear stress: 25 years of bone cell mechanotransduction. J Orthop Res 2009, 27: 143–149.
28 Liu D, Genetos DC, Shao Y, Geist DJ, Li J, Ke HZ and Turner CH, *et al*. Activation of extracellular-signal regulated kinase (ERK1/2) by fluid shear is Ca^{2+}- and ATP-dependent in MC3T3-E1 osteoblasts. Bone 2008, 42: 644–652.
29 Bawin SM and Adey WR. Sensitivity of calcium binding in cerebral tissue to weak electric fields oscillating at low frequency. Proc Natl Acad Sci USA 1976, 73: 1999–2003.
30 Wei LX, Goodman R and Henderson A. Changes in levels of c-myc and histone H2B following exposure of cells to low frequency sinusoidal signals: evidence for window effect. Bioelectromagnetics 1990, 11: 269–272.
31 Luo MY, Song K, Zhang X and Lee I. Mechanism for alternating electric fields induced-effects on cytosolic calcium. Chinese Phys Lett 2009, 26: 0171021–0171024.
32 Shafrir Y and Forgacs G. Mechanotransduction through the cytoskeleton. Am J Physiol Cell Physiol 2002, 282: 479–486.
33 Rubin CT and Lanyon LE. Regulation of bone formation by applied dynamic loads. J Bone Joint Surg 1984, 66: 397–402.
34 Forwood MR and Turner CH. The response of rat tibiae to incremental bouts of mechanical loading: a quantum concept for bone formation. Bone 1994, 15: 603–609.
35 Wang J, Su M, Fan J, Seth A and McCulloch CA. Transcriptional regulation of a contractile gene by mechanical forces applied through integrins in osteoblasts. J Biol Chem 2002, 277: 22889–22895.